XLVI CILAMCE
VITÓRIA - ES - BRAZIL - 2025
XLVI IBERO-LATIN AMERICAN CONGRESS ON COMPUTATIONAL METHODS IN ENGENEERING

# Noise Reduction on Inertial Measurement Unit Sensors in Ballistic Simulators using Deep Models

Noelio Heluy Ferreira, Aleteia Araujo, Flavio de Barros Vidal

*Dept. of Computer Science, University of Brasilia*
*Campus Darcy Ribeiro, 70.910-110, Distrito Federal, Brazil*
*ferreira.noelio@aluno.unb.br, aleteia@unb.br, fbvidal@unb.br*

**Abstract.** This paper introduces a novel approach to stabilizing data from low-cost Inertial Measurement Unit (IMU) sensors. Capitalizing on recent advances in machine learning, the study utilizes a Long Short-Term Memory Recurrent Neural Network (LSTM-RNN) algorithm to mitigate noise caused by electromagnetic interference, which leads to instability and drift in sensor orientation. The proposed method is designed to complement traditional techniques such as noise removal and low-pass filters, providing an initial refinement of the IMU sensor data. By training the model and applying it to dynamic sensor data, the study demonstrates that accuracy can be enhanced through software-based embedded technology, reducing the dependence on expensive high-precision hardware. The findings have significant implications for applications such as simulators (including motion platforms and simulated shooting systems), Unmanned Aerial Vehicles (UAVs), large-scale structural platforms, robotics, and various industrial and engineering contexts.

**Keywords:** Simulation, inertial sensors, IMU, machine learning, LSTM, RNN.

## 1 Introduction

The Brazilian Armed Forces have increasingly adopted military simulation technologies to improve training efficiency, reduce risks, and reduce costs [1]. These systems offer realistic virtual environments and benefit from real-time feedback [2]. Inertial sensors, particularly IMUs, play a central role in both military and civilian domains—ranging from robotics and offshore monitoring to mobile device applications [3].

The integration of IMUs in training improves geolocation, vehicle navigation, and tactical simulations [4]. The Brazilian Army employs simulators like SIMAF and BOMBARDA for artillery exercises [5, 6]. However, IMU drift and the need for frequent recalibration remain key limitations. This study explores the use of Machine Learning and Kalman filters to reduce such errors and meet the precision demands of military applications [7].

This manuscript is organized as follows: Section 2 presents an overview of the theoretical background and related works. Section 3 describes the proposed methodology approach and Section 4 shows all results achieved. Finally, in Section 5 is presented the conclusions and further work.

## 2 Related Works

Inertial Measurement Units (IMUs), composed of accelerometers, gyroscopes, and magnetometers, are fundamental for motion tracking and navigation in various domains such as vehicles, drones, virtual reality, and wearable devices [8]. In Inertial Navigation Systems (INS), IMUs provide continuous acceleration and angular rate data, essential for accurate localization [9]. However, noise, temperature fluctuations, and sensor drift limit their precision, necessitating calibration and advanced filtering techniques [10].

To address such limitations, frequency-weighted Kalman filters have been proposed to suppress noisy frequencies [11], and multi-sensor fusion improves robustness despite individual sensor interferences [12]. Filters such as the Fusion and Noise Removal Filter [13] and Moving Average Filter [14] offer runtime efficiency and smoothing, though insufficient for long-term drift correction.

The Kalman Filter (KF) remains a key tool in state estimation for dynamic systems [15], yet its limitations in addressing cumulative drift motivate hybrid approaches. In this context, Machine Learning, particularly LSTM

networks, has shown promise for enhancing IMU data stability by learning temporal dependencies [16]. CNN-LSTM architectures have been applied effectively in behavior recognition and drift mitigation tasks [17].

Studies demonstrate that LSTM improves performance in MEMS-based IMUs by reducing signal noise and improving tracking accuracy [18]. Its integration with traditional filters offers a robust solution for drift compensation in autonomous systems [19].

A comparative review highlights the widespread use of IMUs [8, 12, 15, 18, 20–26], the application of Kalman filters [12, 15, 18, 20, 21, 26], and the increasing role of LSTM networks [8, 12, 18, 24–26] in military and sensor-based activity recognition. While the moving average filter appears in fewer cases [14], it remains a lightweight option for basic noise reduction. Notably, some studies such as [27] do not adopt any of these techniques, serving as baselines in comparative evaluations.

## 3 Proposed Methodology

This study proposes a hybrid approach combining filtering techniques and machine learning to improve the accuracy and stability of ballistic simulators such as SIMAF[1] and BOMBARDA[2]. The primary goal is to enhance IMU sensor reliability by mitigating noise and drift, thereby improving simulation fidelity.

**Signal Preprocessing.** Based on Valenti *et al.* [13], the Fusion and Noise Removal Filter was adopted to fuse gyroscope and accelerometer data. High-pass filtering of gyroscope signals and low-pass filtering of accelerometer signals allow drift correction and noise suppression. This preprocessing improves attitude estimation and prepares consistent input for training LSTM models.

**Data Collection and Structuring.** Sensor data were collected in controlled and uncontrolled environments using Sensor 1, yielding 2 million records. Additional datasets of 1 million vectors each were collected from Sensors 2 and 3 to evaluate model generalization. The dataset, organized as 3D vectors (X, Y, Z), was filtered and structured as shown in Table 1.

Table 1. Sample Data from Sensor 1.

| **Index** | **X** | **Y** | **Z** |
|---|---|---|---|
| 0 | -0.000950 | 0.000237 | 0.010570 |
| ... | ... | ... | ... |

**Model Training and Evaluation.** The LSTM model was trained on Sensor 1 data (70% training, 30% testing) using the Nadam optimizer for better convergence with noisy signals. The model's hyperparameters were systematically evaluated to determine their impact on performance. Different values for the number of hidden units and layers were tested; however, configurations with additional layers or larger hidden dimensions resulted in inferior performance and were therefore not applied. Similarly, bidirectional architectures and dropout regularization were tested but ultimately discarded due to suboptimal results. The input embedding size was set to 3, corresponding to the $X$, $Y$, and $Z$ components of the input features. Experiments comparing sequence outputs versus final state outputs were also conducted, but the simpler configuration yielded better outcomes. The final model employed a batch size of 608 and a sequence length of 64. Model evaluation was performed using cross-validation to ensure that the temporal order of the observations was preserved throughout training and testing. Evaluation metrics included Mean Squared Error (MSE) and Mean Absolute Error (MAE), with early stopping employed to avoid overfitting. Model performance was further validated using data from Sensors 2 and 3.

**Filtering Pipeline.** Complementary filtering methods were employed for comparison: **Moving Average Filter:** Applied for noise smoothing, though limited by slower response to fast dynamics [14]. **Kalman Filter:** Used for real-time dynamic state estimation under noise. **LSTM Refinement:** Applied post-Kalman filtering for sequential correction of sensor drift and noise.

The proposed pipeline—Fusion Filter → Kalman Filter → LSTM—demonstrated effective stabilization of IMU signals, reducing both short-term fluctuations and long-term drift, thus enabling more reliable ballistic simulation.

## 4 Results

This section presents the results obtained from applying the previously proposed methodology. These results aim to assess the initial effectiveness of the adopted approaches, particularly regarding the stabilization of sensory

[1] `https://casul.eb.mil.br/index.php/simaf`

[2] `http://www.ebrevistas.eb.mil.br/ECO/article/view/6395`

data from SIMAF and BOMBARDA and the generalization capability of the LSTM model.

### 4.1 Comparison Between the Kalman Filter and the Moving Average Filter

Compared to the Moving Average Filter, the Kalman Filter proved to be superior in terms of response to sensor state changes, in addition to the observed stabilization, as shown in Figure 1. On the left side of the Moving Average Filter graph, while the observed angles show a convergence state towards the real value, in the Kalman Filter, the angles already exhibit converged and stabilized values. The convergence speed can be better demonstrated and analyzed on the right side of both graphs, making it possible to infer that the use of the KF was more effective than the MAF.

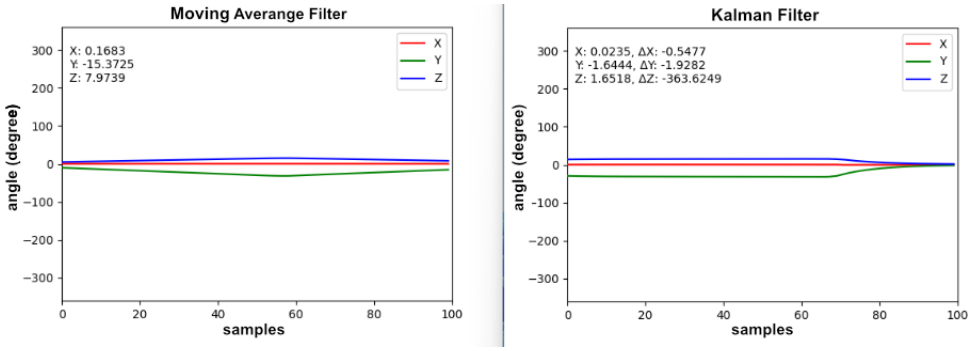



Figure 1. Efficiency Between the Kalman and Moving Average Filters.

### 4.2 Analysis of Model Results on the Test Dataset of Sensor 1

The application of the trained model to the test data from Sensor 1 yielded remarkable results in terms of accuracy and model adequacy. The Mean Squared Error (MSE), a metric that quantifies the average squared differences between predicted and actual values, was extremely low ($MSE = 1.6003762938367268e-07$, $R^2 = 0.9995238874267259$), indicating high prediction accuracy. Furthermore, the coefficient of determination, known as $R^2$, was very close to 1, implying that the model can explain approximately 99.95% of the variance in the test data, as evidenced above. Figure 2 illustrates the comparison between actual values and the values predicted by the model for the X, Y, and Z axes of Sensor 1. This visual alignment reflects the low MSE and the high coefficient of determination $R^2$, demonstrating that the model accurately predicts axis behavior under different conditions over time. In summary, the results from Sensor 1 confirm the effectiveness of the developed model.

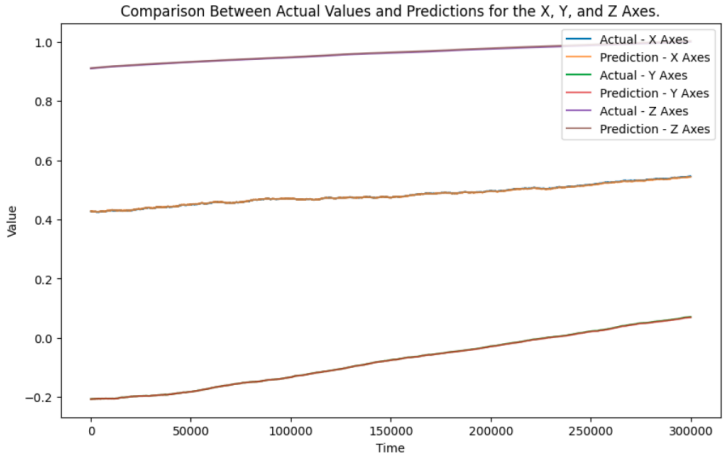


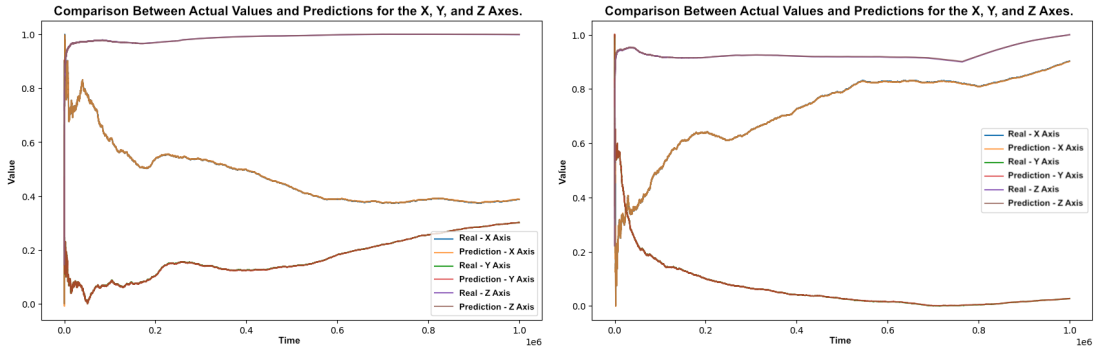

Figure 2. Prediction on test data from Sensor 1 (30%).

### 4.3 Model Validation Analysis on New Data from Sensor 1 in a Different Environment

The validation of the trained model on new data from Sensor 1, collected in a different environment, provided valuable insights into its generalization and robustness. The analysis of these data revealed an MSE ($MSE = 3.839371810655107e{-}07$, $R^2 = 0.9998989761072151$), although slightly higher than that obtained in the original test dataset, it still represents remarkable accuracy in the model's predictions. The coefficient of determination $R^2$, close to 1, suggests that the model can explain approximately 99.99% of the variance in the new data. A high $R^2$ in a different dataset is an indication of the model's effectiveness under varying conditions.

### 4.4 Speculative Analysis of the Application of the Sensor 1 Model to Sensor 2 Data

The application of the model developed for Sensor 1 to Sensor 2 data yielded promising results. The analysis of Sensor 2 data using the Sensor 1 model revealed an MSE ($MSE = 3.378386841031626e - 07$ e $R^2 = 0.9998523721121617$), suggesting that the model can accurately predict Sensor 2 values despite the inherent differences between the sensors.




(a) Prediction for Sensor 1 (new data).

(b) Prediction on test data from Sensor 2.

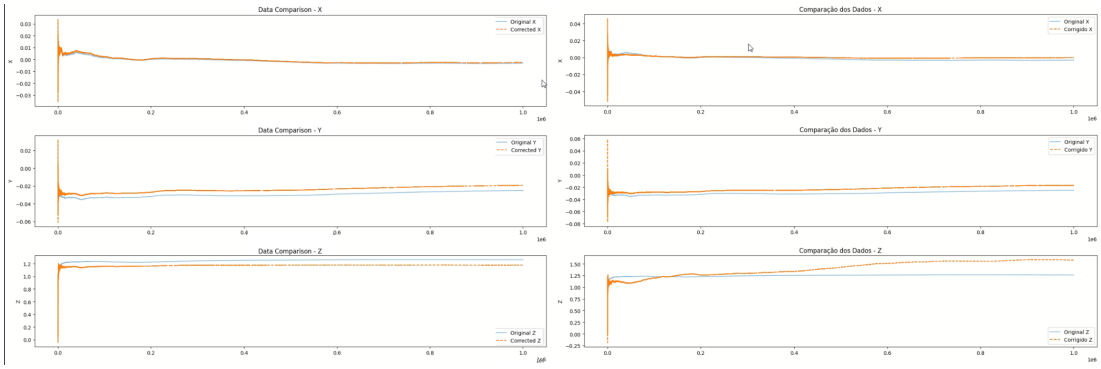
Figure 3. Predictions on new and test data for Sensor 1 and Sensor 2.

The results suggest that the model developed for Sensor 1 has a generalization capability beyond the original training dataset. This indicates that it has learned the fundamental characteristics of inertial sensor data that can be transferred between different devices.

### 4.5 Analysis of Model Application for Sensor Data Stabilization

The model was initially applied to stabilize sensor data concerning long-term drift. The results were favorable for drift correction, with a weight, known as the correction factor, assigned to adjust the model response as needed.

After observing the effect of a 0.7 weight (Figure4a) applied to the Correction Factor, as seen in Figure 4a, comparisons were made with a weight of 1.0, as illustrated in Figure 4b.




(a) Long-term drift correction with Correction Factor = 70.

(b) Long-term drift correction with Correction Factor = 100.

Figure 4. Comparison of long-term drift correction using different correction factors.

### 4.6 Efficiency of the Results

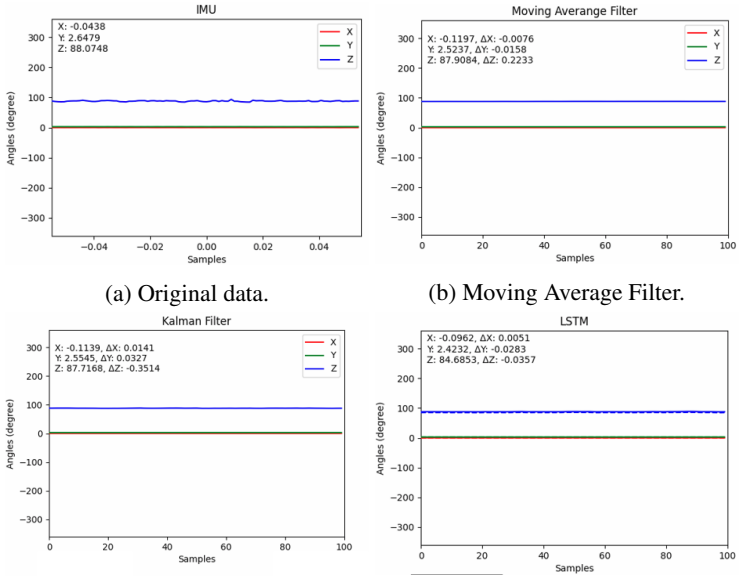
To ensure that the corrections are delivered within the necessary time, it was essential to implement and analyze different filters and algorithms to stabilize the sensory data from the IMU. In the first attempt, when passing the sensor data through the low-pass filter, the Kalman Filter, and then feeding them into the LSTM for additional corrections, an exponential cumulative delay occurred. This delay prevented real-time processing due to buffer accumulation. The optimization of filters and the LSTM significantly reduced processing time. This technique facilitated the tuning of filter and algorithm parameters, including the Moving Average Filter and the Kalman Filter, within the necessary time. Below are the main results of applying the filters and LSTM for data stabilization, focusing on comparative accuracy analyses:

**Raw Data Processing (Original Data).** The first window shows how the data behaves with only the Fusion and Noise Removal Filter implemented in the system, as observed in Figure 5a.

**Moving Average Filter.** It is observed that the abrupt movement, seen in Figure 5b, is not as responsive when processed through the Moving Average Filter.

**Kalman Filter.** The abrupt movement is more responsive when processed through the Kalman Filter, outperforming the Moving Average Filter in both responsiveness and stability, as observed in Figure 5c.

**LSTM Algorithm.** The window displays data processed by the Kalman Filter, which initially corrects short-term instability. These data are then processed by the LSTM, significantly refining data stability, as observed in Figure 5d.




(a) Original data. (b) Moving Average Filter.

(c) Kalman Filter. (d) LSTM in real-time.

Figure 5. Comparison of filtering and prediction methods.

The accuracy, as discussed in this study, is defined as the maximum error the sensor should measure, which must not exceed 2 thousandths above or below the expected value. By closely examining Figure 5d, there are angular variation values $\Delta$ for each axis. Since the accuracy must be at most 2 thousandths, this means that the values of $\Delta$ fall within the expected range, i.e., smaller than $2 * 0.05625^o = 0.1125^o$, as will be analyzed in the following section.

Tables 2a, 2b, and 2c represent an excerpt from an official dataset, with data extracted from existing SIMAF sensors. The data collection was conducted by a qualified engineer *in loco*, with the sensors adapted to the shooting materials, following the same procedures used in a simulation exercise. The excerpt contains only the columns for drift variation and elevation relative to the original drift and elevation, meaning it represents the difference between the initial value and the value collected approximately every 5 minutes. It is observed that the values fluctuate over time due to interference from external noise. Additionally, the variation exceeds the permitted error margin of 2 thousandths in a short period of time.

The results obtained confirm the presence of instability, which justifies the non-use of these sensors. This issue becomes even more evident in Tables 2b and 2c, where the data fluctuates abruptly, making the readings unreliable.

The proposed solution in this study, where data is filtered and undergoes stabilization through the Kalman Filter combined with LSTM, produces results with variability not exceeding 1 thousandth of a radian within the

same time step (See Table 2d). Since this is a proof of concept, verification with the sensor mounted on the same shooting material is necessary. With the obtained and analyzed results, it is now possible to outline the next step of this study, which involves practical application and final validation of the proposed techniques. So far, the approaches employed have proven effective in stabilizing data from low-cost inertial sensors, achieving the goal of increasing accuracy without requiring additional hardware. However, to consolidate these findings and fully integrate them into the SIMAF and BOMBARDA systems, it is necessary to proceed to the final phase of this study, where detailed comparisons will be conducted between the developed methods and legacy approaches.

Table 2. Drift and Elevation Variations for GUN03, GUN04, GUN05, and the Proposed Approach (thousandths).

(a) GUN03

| Drift Variation | Elevation Variation |
|---|---|
| 5.6521 | 1.5389 |
| 5.7067 | 1.1315 |
| 5.0848 | 1.1315 |
| 3.0183 | 2.1501 |
| 3.3340 | 5.1040 |
| 4.0639 | 3.5761 |

(b) GUN04

| Drift Variation | Elevation Variation |
|---|---|
| 164.2941 | 112.1580 |
| 17.5273 | -0.3964 |
| 16.9576 | 2.2520 |
| 17.3974 | -0.8038 |
| -1.7740 | 8.2616 |
| -2.3822 | 8.2616 |

(c) GUN05

| Drift Variation | Elevation Variation |
|---|---|
| 11.2151 | -4.0633 |
| 11.1160 | -3.3503 |
| 11.7320 | -3.1466 |
| 11.2617 | -3.6559 |
| 11.1957 | -3.1466 |
| -6.6786 | 5.6133 |

(d) Proposed Approach

| Drift Variation | Elevation Variation |
|---|---|
| 0.0485 | 0.0038 |
| 0.1055 | 0.0044 |
| 0.1900 | -0.0008 |
| 0.2548 | -0.0057 |
| 0.3205 | -0.0103 |
| 0.3839 | -0.0104 |
| 0.4587 | -0.0084 |
| 0.5257 | -0.0049 |
| 0.5994 | -0.0040 |

## 5 Conclusion and Future Work

The accuracy of the simulator exercises, in terms of human errors in weapon data recording, ranged from -2”’ to +2”’ (thousandths), equivalent to 0.1125º. The obtained results met the simulation requirements; however, further *in loco* testing is necessary to validate and refine these findings.

The integration of high-pass and low-pass filters with the LSTM algorithm showed significant potential in stabilizing low-cost inertial sensors. Although the results are promising, additional testing is required to achieve higher reliability, depending on the application. Concurrent processing, though secondary, played a crucial role in enabling seamless integration of filters and algorithms without delays from buffer accumulation. This advancement supports real-time analysis of statistical or machine learning-based filters, using identical or distinct datasets independently or in combination, making it particularly useful for laboratory bench testing. This study represents a step forward in improving the accuracy of low-cost IMU sensors, but does not take all the possibilities into account. Ongoing experimentation and adaptation are essential to meet the evolving demands of real-time applications.

Future work will focus on refining these methodologies, expanding real-world testing, and exploring hybrid approaches that integrate traditional filtering with deep learning techniques to further enhance IMU sensor accuracy.

**Authorship statement.** The authors hereby confirm that they are the sole liable persons responsible for the authorship of this work, and that all material that has been herein included as part of the present paper is either the property (and authorship) of the authors, or has the permission of the owners to be included here.

## References

[1] V. Savchenko, A. Y. Derevjanchuk, T. Dzyuba, and D. Moskalenko. Intensive training model for artillery cadets using 3d simulators. *Advances in Military Technology*, 2023.
[2] L. F. S. Wilin. O simulador de apoio de fogo e a influência no adestramento de tropas. *Revista Doutrina Militar Terrestre*, vol. 9, n. 28, pp. 56–61, 2021.
[3] D. Ryumin, D. Ivanko, and E. V. Ryumina. Audio-visual speech and gesture recognition by sensors of mobile devices. *Sensors (Basel, Switzerland)*, vol. 23, 2023.
[4] S. Bultmann, R. Memmesheimer, and S. Behnke. External camera-based mobile robot pose estimation for collaborative perception with smart edge sensors. *ICRA 2023*, pp. 8194–8200, 2023.
[5] E. Brasileiro. Caderno de instrução emprego da simulação. edição experimental. itens 3.2.3, 2020.
[6] D. d. N. Duarte. Proposta de metodologia de emprego do sistema de simulação de apoio de fogo no adestramento dos pelotões de morteiro pesado. *Biblioteca do Exército*, 2020.
[7] de H. Oliveira Gressler. DIEx 29-DACDS-SMA/DACDS/CDS. Relatório Técnico EB: 64202.004463/2024-32, Exército Brasileiro, Destacamento Avançado do DCT em Santa Maria, Brasília, DF. Documento assinado eletronicamente, 2024.
[8] J. Zhao and E. Obonyo. Convolutional long short-term memory model for recognizing construction workers' postures from wearable inertial measurement units. *Advanced Engineering Informatics*, vol. 46, pp. 101177, 2020.
[9] A. E. Mahdi, A. Azouz, A. E. Abdalla, and A. Abosekeen. A machine learning approach for an improved inertial navigation system solution. *Sensors*, vol. 22, n. 4, pp. 1687, 2022.
[10] M. Mundt, W. R. Johnson, W. Potthast, B. Markert, A. Mian, and J. Alderson. A comparison of three neural network approaches for estimating joint angles and moments from inertial measurement units. *Sensors*, vol. 21, n. 13, pp. 4535, 2021.
[11] A. Shaghaghian and P. Karimaghaee. Accuracy improvement in motion-measurement using frequency-weighted kalman filter. *IET Radar, Sonar & Navigation*, vol. 14, n. 1, pp. 89–96, 2020.
[12] S. Hosseinyalamdary. Deep kalman filter: Simultaneous multi-sensor integration and modelling; a gnss/imu case study. *Sensors (Basel, Switzerland)*, vol. 18, n. 5, pp. 1316, 2018.
[13] R. G. Valenti, I. Dryanovski, and J. Xiao. Keeping a good attitude: A quaternion-based orientation filter for imus and margs. *Sensors*, vol. 15, n. 8, pp. 19302–19330, 2015.
[14] H. Xue, M. Ruan, and Y. Cheng. A fixed length adaptive moving average filter-based synchrophasor measurement algorithm for p class pmus. *Energies*, vol. 12, n. 21, 2019.
[15] C. Montella. The kalman filter and related algorithms: A literature review. *Journal of Algorithmic Finance*, 2011.
[16] I. Goodfellow, Y. Bengio, and A. Courville. *Deep Learning Book*. MIT Press, 2017.
[17] F. Saidi and Z. Trabelsi. A hybrid deep learning-based framework for future terrorist activities modeling and prediction. *Egyptian Informatics Journal*, vol. 23, n. 3, pp. 437–446, 2022.
[18] X. Guang, Y. Gao, P. Liu, and G. Li. Imu data and gps position information direct fusion based on lstm. *Sensors*, vol. 21, n. 7, pp. 2500, 2021.
[19] T. Bikmukhametov. How to reshape data and do regression for time series using lstm. -. Accessed: 2023-05-09, 2020.
[20] S. Han, Z. Meng, O. Omisore, T. Akinyemi, and Y. Yan. Random error reduction algorithms for mems inertial sensor accuracy improvement—a review. *Micromachines*, vol. 11, n. 11, pp. 1021, 2020.
[21] S.-H. Won, F. Golnaraghi, and W. Melek. A fastening tool tracking system using an imu and a position sensor with kalman filters and a fuzzy expert system. *IEEE transactions on industrial electronics (1982)*, vol. 56, n. 5, pp. 1782–1792, 2009.
[22] C. Jiang, S. Chen, Y. Chen, B. Zhang, Z. Feng, H. Zhou, and Y. Bo. A mems imu de-noising method using long short term memory recurrent neural networks (lstm-rnn). *Sensors*, vol. 18, n. 10, pp. 3470, 2018.
[23] D. Nagaraj, E. Schake, P. Leiner, and D. Werth. An rnn-ensemble approach for real time human pose estimation from sparse imus. In *3rd Intl Conf on App of Intelligent Systems*, pp. 1–6, 2020.
[24] F. Meißl, F. Eibensteiner, P. Petz, and J. Langer. Online handwriting recognition using lstm on microcontroller and imu sensors. In *ICMLA 2022*, pp. 999–1004. IEEE, 2022.
[25] T.-H. S. Li, P.-H. Kuo, C.-H. Cheng, C.-C. Hung, P.-C. Luan, and C.-H. Chang. Sequential sensor fusion-based real-time lstm gait pattern controller for biped robot. *IEEE Sensors Journal*, vol. 21, n. 2, pp. 2241–2255, 2020.
[26] Y. Zhang. A fusion methodology to bridge gps outages for ins/gps integrated navigation system. *IEEE Access*, vol. 7, pp. 61296–61306, 2019.
[27] H. d. O. Gressler and M. C. Cera. O impacto da paralelização com openmp no desempenho e na qualidade das soluções de um algoritmo genético. *Revista Brasileira de Computação Aplicada*, vol. 6, pp. 35–47, 2014.